Structure and Morphogenesis of the Frustule

Iaroslav Babenko, Benjamin M. Friedrich, and Nils Kröger

Abstract

The intricate morphology of diatom cell walls has fascinated scientists since the invention of the light microscope more than 300 years ago. However, it was not recognized until 1844 that the diatom cell wall, termed frustule (from Latin *frustulum* = piece, chunk), is actually mainly composed of glass (amorphous SiO_2 or silica). As more and more details of frustule structures from numerous species were revealed through improvements in light microscopy and the development of electron microscopy, it became increasingly mysterious as to how such amazingly complex inorganic architectures are produced by individual cells. The species-specificity of the frustule structure indicates that the blueprint for its morphogenesis is encoded in adiatom's genome. Unveiling the machinery that executes this morphogenesis program is still ongoing (see also Chap. "Biomolecules Involved in Frustule Biogenesis and Function"). Here, we explain the general architectures of frustules and describe the main cellular events and key steps in their morphogenesis.

I. Babenko
B CUBE, Center for Molecular and Cellular Bioengineering, TU Dresden, Dresden, Germany

Cluster of Excellence Physics of Life, TU Dresden, Dresden, Germany

cfaed, TU Dresden, Dresden, Germany

B. M. Friedrich
Cluster of Excellence Physics of Life, TU Dresden, Dresden, Germany

cfaed, TU Dresden, Dresden, Germany

N. Kröger (✉)
B CUBE, Center for Molecular and Cellular Bioengineering, TU Dresden, Dresden, Germany

Cluster of Excellence Physics of Life, TU Dresden, Dresden, Germany

Faculty of Chemistry and Food Chemistry, TU Dresden, Dresden, Germany
e-mail: nils.kroeger@tu-dresden.de

A. Falciatore, T. Mock (eds.), *The Molecular Life of Diatoms*,
https://doi.org/10.1007/978-3-030-92499-7_11

Keywords

Diatoms · Frustule · Morphogenesis · Architecture

Abbreviations

ER	Endoplasmic reticulum
GFP	Green fluorescent protein
MC	Microtubule organizing center
Mya	Million years ago
PSS	Primary silicification site
SDV	Silica deposition vesicle
SEM	Scanning electron microscopy
TEM	Transmission electron microscopy
VHA	V-type H^+-ATPase

1 Frustule Architecture

The name diatom originates from the Greek word *diatomos,* which means "two parts," indicating that each frustule is composed of two pieces, which together fully encase the protoplast. Each piece is termed *theca* (Greek for box, case) and both thecae generally possess identical geometries but differ slightly in size. One theca, termed *epitheca*, is slightly larger than the other one, termed *hypotheca*. The two thecae fit into each other like the two halves of a Petri dish with a narrow overlap (Fig. 1).

Each theca consists of a valve and several rings (or sometimes short strips) of silica termed girdle bands. Together, the girdle bands form the *cingulum* (Latin for girdle). Girdle bands usually have a relatively simple architecture with a smooth surface and a regular pattern of pores. Valves are generally much more intricately patterned, comprising a meshwork of silica ribs and hierarchically arranged pore patterns. Together, the valve and the girdle bands form a connected structure where neighboring silica elements overlap rather than being fused with each other. The terminal girdle bands of each theca constitute the region where the epi- and hypotheca overlap.

Diatoms are classified as either centrics or pennates according to frustule symmetry with respect to the pervalvar axis (see Fig. 1). *This classification is not evolutionary meaningful, as according to phylogenetics pennates form a monophyletic group together with the polar centrics and thus are not an independent evolutionary invention* (Sims et al. 2006). Pennates have bilateral symmetry, characterized by an elongated valve (Fig. 2a) that defines an apical axis running between the two poles of the valve (see Fig. 1). There are two different types of pennates depending on whether the valve contains a *raphe* (raphid pennates) or not (araphid pennates). A

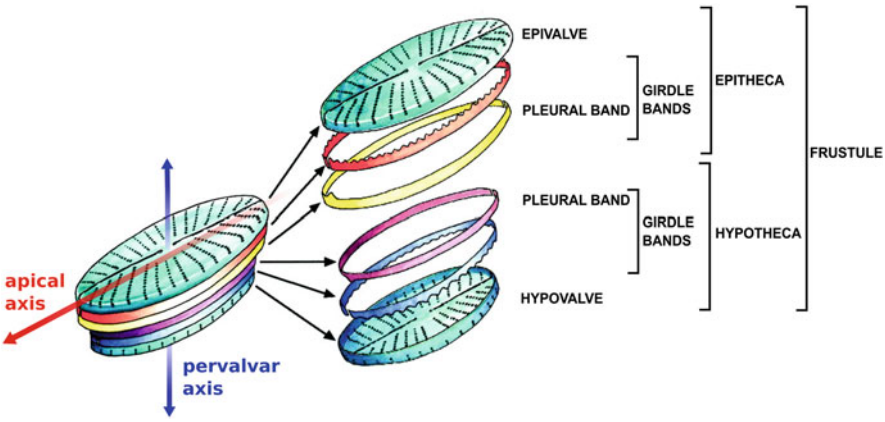

Fig. 1 Frustule architecture. Adapted from Zurzolo and Bowler (2001). Reprinted with permission

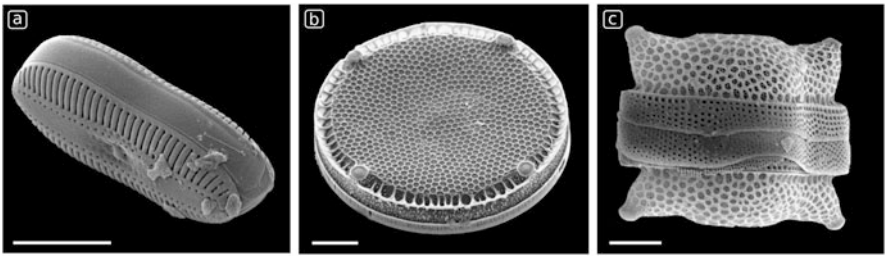

Fig. 2 Scanning electron microscopy (SEM) images of (**a**) the raphid pennate *Diploneis sp*., (**b**) the radial centric *Eupodiscus radiatus* and (**c**) the bipolar centric *Biddulphia reticulata*. Scale bars (**a**, **c**): 10 μm, (**b**): 20 μm. Adapted from Bradbury (2004). Reprinted with permission

raphe (Greek for seam) is a system comprising two elaborate slit-like structures bordered by two thick ribs that run along the apical axis, although sometimes there is only one slit (especially in Bacillariaceae). Araphid pennates have a single axial rib structure that lacks slits. Centrics are divided into radial centrics with radial symmetry around the pervalvar axis (Fig. 2b), and polar centrics characterized by three-, four-, or five-fold symmetry (Fig. 2c). Centrics are evolutionarily older than pennates (Girard et al. 2009) and both groups differ in their life cycle strategies (see Chap. "Life Cycle Regulation"). The earliest fossil records of centric diatoms stem from the Lower Cretaceous 100–145 million years ago (Mya) (Sims et al. 2006), whereas the raphid pennate group does not appear before the middle Eocene 46-77 Mya (Sims et al. 2006; Gladenkov 2012).

1.1 Centrics

The valves of centric diatoms generally contain highly regularly arranged pores, which often exhibit a hexagonal pattern (Fig. 3a). Such patterns may actually exhibit two to four hierarchical levels of pores that generally maintain the same symmetry of arrangement on each level (Fig. 3b), although exceptions exist. In some species, including the model diatom *Thalassiosira pseudonana*, pores are arranged in a seemingly irregular fashion (Fig. 3c). The pores in the first hierarchical level are termed *loculate areola* (Latin for small open space), which are cylindrical punctures of the valve (Fig. 4d). The two openings of each areola are morphologically distinct (Fig. 4, schematic).

One opening is unoccluded and is termed the *foramen* (Latin for opening), while the other opening is sealed by a thin layer of silica termed the *cribrum* layer (Latin for sieve), which is perforated with many smaller pores, termed cribrum pores. The cavity inside an areola pore is referred to as *loculus*. The size of cribrum pores varies from species to species, ranging from ~300 nm like in *Coscinodiscus asteromphalus* to ~20 nm as in *T. pseudonana.* Cribrum pores themselves can be sub-patterned by yet a third hierarchical level of pores called *cribrellum* (Fig. 4c) (Round et al. 1990; Romann et al. 2015). The orientation of the foramen layer and the cribrum layer is a taxonomic criterion. For example, in *C. asteromphalus,* foramina are on the proximal side (i.e. facing towards the cell center) and the cribrum layer on the distal side (i.e. facing away from the cell center), whereas it is the other way around in *Thalassiosira eccentrica.*

Many centric diatoms possess two types of tube-shaped biosilica structures that project through the valve, called *fultoportula* (or strutted process) and *rimoportula* (or labiate process). Fultoportulae are present only in some species of the order *Thalassiosirales* and consist of a central tube that passes through the valve with two

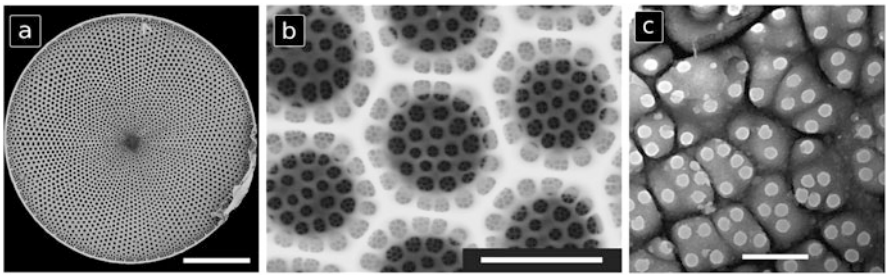

Fig. 3 Electron micrographs of valves from different centric diatoms. (**a**) SEM image of a *Coscinodiscus perforatus* valve showing a highly regular hexagonal pattern of pores throughout the valve (from Sar et al. 2010). Reprinted with permission. (**b**) SEM image of a detailed view of the valve of *Coscinodiscus radiatus,* which contains three hierarchical layers of hexagonal pore patterns (from Sumper 2002). Reprinted with permission. (**c**) Detailed view of a transmission electron microscopy (TEM) image of the *Thalassiosira pseudonana* valve displaying irregular pattern of pores (courtesy of Stefan Görlich, TU Dresden). Scale bars (**a**): 50 µm, (**b**): 2.5 µm, (**c**): 0.2 µm

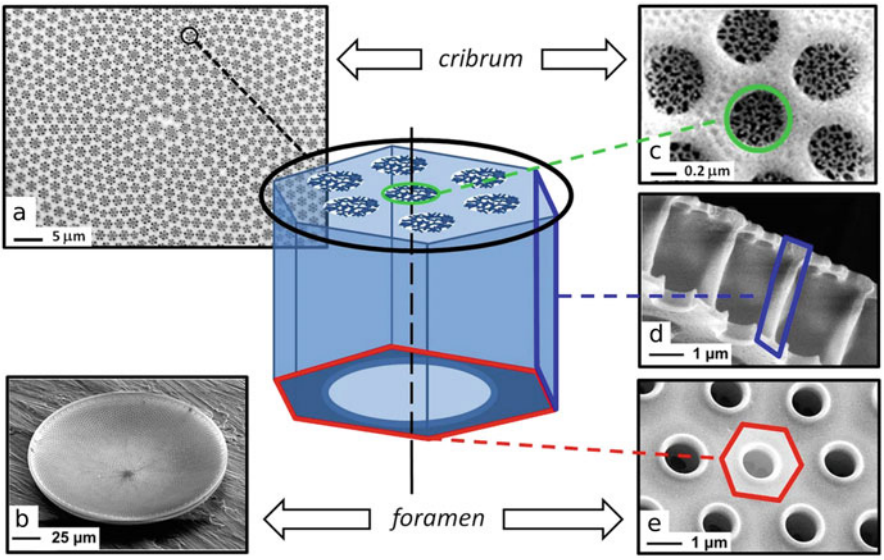

Fig. 4 SEM images of hierarchically arranged pores in *Coscinodiscus centralis* valves. The schematic in the middle highlights the 3D arrangement of the pore patterns. (**a**) Distal side, (**b**) proximal side, (**c**) cribrum layer (distal side) with two hierarchical levels of pores. (**d**) Side view of a fractured valve. (**e**) Layer of foramina. From Romann et al. (2015). Reprinted with permission

to four subsidiary tubes (satellite tubes) symmetrically arranged around the central tube. The distal domain of the central tube can appear as an emphasized pore with a thick silica rim (Fig. 5a, red arrow). The satellite pores are only visible on the proximal face of the valve (Fig. 5b, red arrow). Fultoportulae can be positioned near the center of the valve, where they may be solitary or form small clusters, or be regularly spaced in a ring-like arrangement near the valve margin. They function as secretion sites for β-chitin fibers that are synthesized by as yet uncharacterized, plasma membrane-bound chitin synthase complexes positioned right beneath each fultoportula (Herth and Schnepf 1982; Durkin et al. 2009; LeDuff and Rorrer 2019). The β-chitin fibers are known to increase the hydrodynamic resistance of the diatom cell, thus slowing down its sinking rate (Eppley et al. 1967; Walsby and Xypolyta 1977). In some species (e.g. *Thalassiosira rotula*) the chitin fibers are required for colony formation, where they provide physical links between neighboring cells (Round et al. 1990). Rimoportulae are found in almost all centric species and also some pennates (mostly in araphid genera). Each rimoportula commonly appears as a simple pore on the distal side (usually larger than an areola), and exhibits a pair of lip-like silica structures on the proximal surface (Fig. 5b, blue arrow). The biological function of rimoportulae has remained unknown so far, but it has been speculated that they are involved in osmoregulation (Schulz et al. 1984). There are several reports on motile centric and araphid diatoms, and it was suspected that rimoportulae

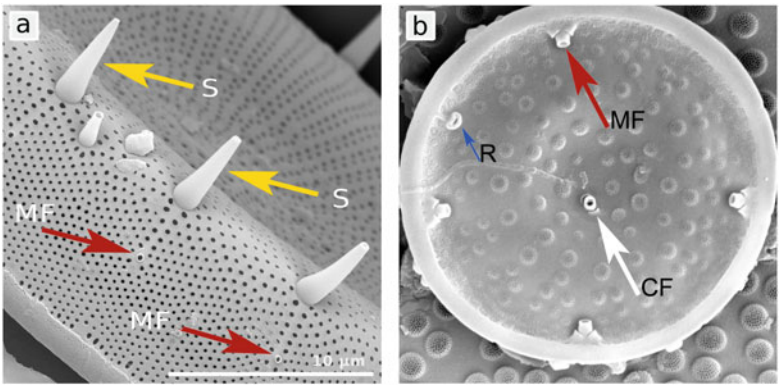

Fig. 5 SEM images of tubular processes. (**a**) Distal valve side of *Stephanodiscus yellowstonensis*, and (**b**) proximal valve side *Stephanodiscus sp*. A row of spines (S, yellow arrow) consisting of conical protrusions. A rimoportula (R, blue arrow) is a lip-like structure on the proximal side of the valve. A marginal fultoportula (MF, red arrow) is positioned near the rim of the valve, and a central fultoportula (CF, white arrow) is in or close to the valve center. In each fultoportula, only the central tube is visible on the distal surface, whereas the satellite tubes (here: two) can only be seen on the proximal side. Adapted from Spaulding and Potapova (2020). Courtesy of Sarah Spauling

are involved in driving cell motility in these species (Medlin et al. 1986; Pickett-Heaps et al. 1990; Sato and Medlin 2006).

1.2 Pennates

Pennate diatoms owe their name to the Latin word *penna*, which means feather and refers to the architecture of their valves with a central rib and usually orthogonal branches resembling the vane of a feather. The two subgroups, raphid and araphid pennates, are distinguished according to the morphology of the central rib structure, which extends almost entirely along the apical axis of the valve. In the majority of raphid pennate species, the central rib has two slits (also termed fissures) that are (in most cases) interrupted by the central nodule, a heavily silicified structure positioned in the middle of the *sternum* (Fig. 6a, b). This system of slits is termed *raphe* and is essential for the gliding motility of raphid diatoms (see Chap. "Diatom Adhesion and Motility"). While most raphid pennates contain a raphe in both valves, some species are monoraphid with one valve being rapheless. The sternum of araphid pennates is less conspicuous than in raphid pennates and lacks the fissures. Due to the absence of a raphe system, araphid pennates are nonmotile (with a few exceptions, see above and Chap. "Diatom Adhesion and Motility"). The valves of most araphid pennates contain an unornamented region termed the *hyaline* or the valve center, which lacks pores or tubes, and appears as a smooth silica domain on the distal and proximal surface of valves (Fig. 6c, e). The valves of pennates possess areola pores, which are fairly uniformly sized and organized in regularly spaced

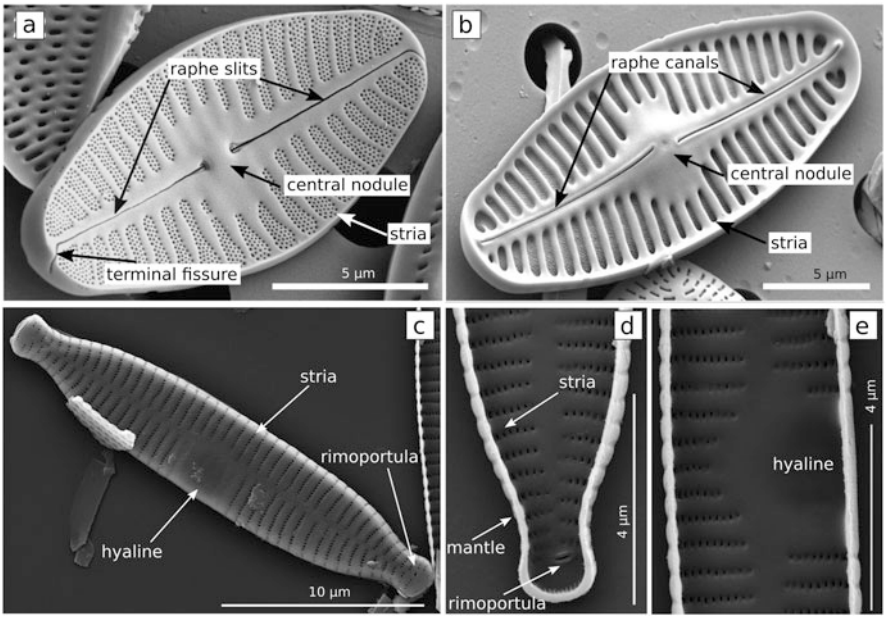

Fig. 6 SEM micrographs of (**a**, **b**) raphid and (**c**–**e**) araphid pennates. (**a**) Distal and (**b**) proximal valve surface of the raphid pennate *Planothidium bagualensis* containing a raphe system. (**c**) Distal and (**d**, **e**) proximal valve surface of the araphid pennate *Fragilaria recapitellata*. From Wetzel and Ector (2014), Bishop and Spaulding (2014). Reprinted with permission

rows termed *striae* (Latin for grooves; Fig. 6a–d). While the areola pores of centrics are generally circular, in pennates they are often oval or slit-like. The areola pores of pennates may be covered by one or two thin, porous layers of silica termed occlusions, which is a feature that they share with many centrics.

The ability to actively move towards favorable conditions or away from unfavorable conditions endows raphid diatoms with a considerable advantage over nonmotile species. However, the fissures of the raphe system severely compromise the mechanical stability of the frustule. Therefore, three countermeasures have evolved: (i) the raphe system is heavily silicified, (ii) the cross-sections of the raphe slits are usually S-shaped such that one raphe rib fits like a notch into the other rib (see Chap. "Diatom Adhesion and Motility"), and (iii) the formation of silica bridges (called *fibulae*) that link the two sides of the valve beneath the raphe (most prominent in Bacillariaceae and Surirellaceae).

2 Frustule Biogenesis

In 1964 it was discovered that silica formation in diatoms is an intracellular rather than extracellular process (Drum and Pankratz 1964). The silica parts of the frustule, valves, and girdle bands are produced in individual vesicles and, when completed,

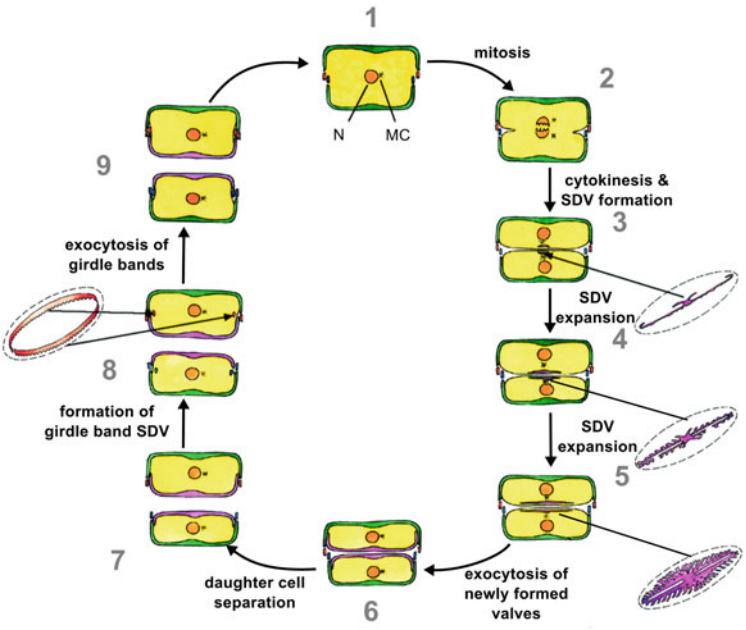

Fig. 7 Schematic of the diatom cell cycle. Transapical sections of a cell at different cell cycle stages (numbers 1–9) are shown. The purple and red drawings labeled "SDV" represent oblique views of different developmental stages of valve morphogenesis and a girdle band near completion, respectively. N = nucleus, MC = microtubule organizing center, SDV = silica deposition vesicle. From Zurzolo and Bowler (2001). Reprinted with permission

released to the cell surface (Fig. 7). Biogenesis of the silica forming vesicles is strictly regulated by the cell cycle. Cytoskeleton fibers and vesicles of unknown origin are usually in immediate proximity to the silica deposition vesicles, yet the molecular underpinnings and mechanisms that link vesicle transport and cytoskeletal dynamics to silica biogenesis are so far unknown. In this section, we summarize the cytoplasmic events that have been observed during frustule biogenesis, while Sect. 3 below will describe events that take place inside the silica forming vesicles.

2.1 Cell Cycle Control of Silica Biogenesis

Following mitosis, cytokinesis occurs precisely in the mid-cell region parallel to the valves. The resulting two daughter protoplasts remain enclosed within the parental frustule (Fig. 7, stages 1–3). Shortly after cytokinesis, a new valve forms inside an expanding disk-shaped silica deposition vesicle (SDV) in each protoplast right next to their plane of contact (Fig. 7, stages 3–5). When morphogenesis of an entire valve is completed, the valve SDV undergoes exocytosis, thus depositing the newly formed valve in the contact zone between the protoplasts (Fig. 7, stages 5–6).

After exocytosis, the two daughter cells separate, each inheriting a theca from the parent cell to which a new valve has been added, thus being equipped with a frustule that completely encases the protoplast (Fig. 7, stages 6–7). During interphase, protoplast growth requires the sequential synthesis of a species-specific number of new girdle bands to avoid gaps within the frustule as the protoplast enlarges (Fig. 7, stages 7–9). Each girdle band is produced within an individual SDV that is positioned precisely in the mid-cell region just below the margin of the hypotheca (Fig. 7, stage 8). After completion of morphogenesis of the first girdle band, the SDV undergoes exocytosis and the girdle band added onto the edge of the new valve (Fig. 7, stage 9). Only after exocytosis, a new girdle band SDV is formed in the mid-cell region, and the resulting second girdle band is added to the edge of the first one through exocytosis. This sequential process of girdle band formation continues until the protoplast has reached the critical size for the next cell division (Fig. 7, stages 9–1).

The petri-dish like stacking of the two thecae in a frustule has the consequence that a diatom cell population will gradually decrease in average size with each cell generation (McDonald-Pfitzer rule). During cell division, the hypotheca of the mother cell, which is slightly smaller than the epitheca (see Fig. 1), becomes the epitheca of one of the daughter cells (Fig. 7, bottom cell). The daughter cell then produces a new hypotheca that has to be smaller than the inherited hypotheca of the mother cell. To prevent shrinking down to unviable sizes, three mechanisms have evolved:

1. Sexual reproduction allows diatoms to restore their species-specific maximum cell size. The sexual phase is triggered once cells reach a critical size threshold, which is a characteristic for each species. After meiosis, the gametes fuse, yielding a zygote (called auxospore), which sheds its frustule and drastically increases in size. The enlarged auxospore then resumes frustule formation, producing large, frustule-encased cells (see Chap. “Life Cycle Regulation”).
2. There are a few records showing that some centric (Nagai et al. 1995) and some pennate species (Sato et al. 2008) have evolved an asexual mechanism for size restoration that is similar to sexual reproduction. Here, an auxospore-like cell (“uniparental auxospore”) sheds its frustule without having undergone meiosis. *De novo* formation of a new frustule generates much larger frustule-encased cells as in (i). How biogenesis of the asexual auxospore-like cell is achieved, is not yet understood.
3. Some centric diatoms, including the model diatom *T. pseudonana*, are known to form auxospores or auxospore-like cells (Moore et al. 2017). How these species avoid size reduction has remained somewhat mysterious. Maintenance of a viable cell size in some species is probably achieved by the ability to occasionally produce expandable girdle bands that have larger diameters than the hypovalve (Geitler 1932; Hildebrand et al. 2007).

2.2 Silica Deposition Vesicles

Electron microscopy studies have clearly demonstrated that valve and girdle band formation is entirely accomplished within the corresponding SDVs (for a review see Pickett-Heaps et al. 1990). The membrane of the SDV is termed *silicalemma* and in TEM analysis of sectioned cells displays a typical lipid bilayer structure. SDVs are not unique to diatoms, but are also present in all other silica forming protists like radiolarians, choanoflagellates, bolidophytes and sponges to name but a few (Simpson and Volcani 2012). From biochemical analysis of mature frustules and transcriptomics analyses of synchronized cells, proteins and other organic components were identified that are also present in SDVs (Kotzsch et al. 2017; Tesson et al. 2017). This provided valuable insights into understanding of diatom silica deposition on a molecular level (see Chap. "Biomolecules Involved in Frustule Biogenesis and Function" for details).

It has been suggested that SDVs are formed by the fusion of vesicles that originate either from the Golgi apparatus (Dawson 1973; Schmid et al. 1981), or from the endoplasmic reticulum (ER) (Hoops and Floyd 1979; Schmid et al. 1981; Chiappino and Volcani 1977). In the centric diatom *T. eccentrica,* small vesicles of 30–40 nm in diameter were observed to accumulate around the valve SDV, presumably delivering new material for valve SDV expansion (Schmid and Schulz 1979; Schmid et al. 1981). The diameter of these vesicles resembled that of transport vesicles of the Golgi apparatus. Also in other diatoms, numerous cytoplasmic vesicles, which seemed to emanate from the Golgi apparatus were observed during valve formation (Round et al. 1990). However, the origin of the presumed transport vesicles remained speculative. The fact that a newly synthesized diatom theca can be stained by acidotropic dyes indicates that the pH in the lumen of the SDV is acidic (Vrieling et al. 1999). Recently, a silicalemma bound V-type H^+-ATPase (VHA) has been discovered that is presumed to be responsible for acidification of the SDV (Yee et al. 2020). VHA is also located in the vacuole (Yee et al. 2020), indicating that either the vacuole or SDV exchange material via vesicle transport, or that both receive material from the same source.

SDV-mediated exocytosis is a remarkable event, because it affects a substantial fraction of the total plasma membrane of the cell (~30% for the valve SDV). In analogy to other vesicle-mediated exocytosis processes known to date, it is to be expected that SDV exocytosis involves fusion of parts of the silicalemma with the plasma membrane, thereby delivering the vesicle content (valve, girdle band) to the cell surface. So far, electron microscopy failed to capture the silicalemma-plasma membrane fusion process, possibly because it may be very short lived. The fate of the silicalemma after exocytosis has thus far remained a conundrum. Four scenarios were suggested (Pickett-Heaps et al. 1990): (1) fusion of the proximal silicalemma with the plasma membrane and secretion of vesicles consisting of the distal silicalemma and the plasma membrane in the region of exocytosis; (2) the distal silicalemma and the plasma membrane in the region of exocytosis become an organic coat around the distal surface of the biosilica; (3) the entire silicalemma and the plasma membrane in the region of exocytosis become an organic coat around

the biosilica, and new plasma membrane is delivered by the endomembrane system; (4) the distal silicalemma temporarily fuses with the plasma membrane, and eventually the entire silicalemma is retrieved into the cytoplasm as endocytic vesicles. Recently, time-lapse fluorescence microscopy imaging of *T. pseudonana* cells expressing silicalemma proteins (Sin1, VHA) tagged with green fluorescent protein (GFP) confirmed the fusion of silicalemma and plasma membrane (Kotzsch et al. 2017; Yee et al. 2020). Quantitative analysis of Sin1-GFP localization during valve biogenesis seemed to rule out scenarios (1) and (3), and was consistent with scenario (4) although insufficient silicalemma material appeared to be retrieved back into the cytoplasm (Kotzsch et al. 2017).

2.3 Cytoskeleton

Experiments with microtubule inhibitors like colchicine (Schmid 1980, Pickett-Heaps et al. 1990, Kharitonenko et al. 2015), podophyllotoxin (Blank and Sullivan 1983), oryzalin (Van de Meene and Pickett-Heaps 2004), and paclitaxel (Bedoshvili et al. 2018), or microfilament inhibitors like cytochalasin D (Van de Meene and Pickett-Heaps 2004; Tesson and Hildebrand 2010b) caused structural anomalies in the silica patterns of the frustules of the inhibitor-treated cells. Although side-effects of drug treatment via compromised cell viability cannot always be excluded, the results clearly indicate that cytoskeletal filaments play a role in silica morphogenesis. This is in line with TEM and fluorescence microscopy of chemically fixed cells, where cytoskeletal filaments were found to co-localize with valve SDVs, as summarized in the following paragraphs (Pickett-Heaps et al. 1990; Tesson and Hildebrand 2010a, b; Cohn et al. 1989; Van De Meene and Pickett-Heaps 2002).

2.3.1 Microtubules

In many diatom species, the nucleus and the microtubule organizing center (MC) are positioned in the immediate vicinity of the valve SDV already at the beginning of SDV development (Pickett-Heaps et al. 1990). TEM analysis of embedded and sectioned cells and immunofluorescence microscopy have shown that in most pennate and centric diatoms, the nucleus and MC are positioned precisely at the center of the proximal side of the developing valve SDV. Numerous microtubules or bundles of microtubules emanate from the MC and extend over the entire proximal surface of the valve SDV (Fig. 8) (Pickett-Heaps et al. 1990; Tesson and Hildebrand 2010a, b). However, although electron and fluorescent microscopy studies provide morphological correlations between microtubules and the newly forming valve, they cannot prove that microtubules directly guide silica morphogenesis. Therefore, the effects of microtubule inhibitors have been studied. Treatment of the centric diatom *Aulacoseira islandica* with a subtoxic concentration of colchicine (preventing polymerization of tubulin) resulted in formation of an ectopic lateral valve located in the girdle band region (Bedoshvili et al. 2018). In pennate diatoms, subtoxic concentrations of colchicine caused raphe displacement, morphological anomalies

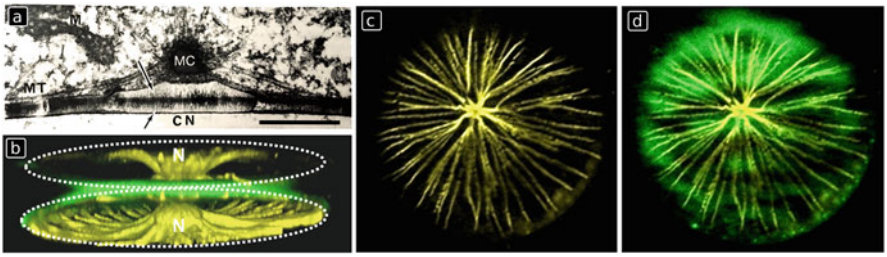

Fig. 8 Locations of nucleus, mictotubule organizing center, and microtubules during valve SDV development. (**a**) TEM image of a longitudinal section of the pennate diatom *Pinnularia viridis*. The microtubule organizing center (MC) is located next to the central nodule (CN) of the newly forming valve (arrows). Microtubules emanate from the MC, extending over the densely silicified zone of the new valve. M – mitochondrium. Scale bar: 0.1 μm. From Pickett-Heaps et al. (1979). (**b**–**d**) Immunofluorescence microscopy in *Coscinodiscus granii* using an anti-tubulin antibody. (**b**) Three-dimensional reconstruction of the microtubule pattern (yellow) and the forming valve (green) shortly after cytokinesis (the dots outline the two daughter cells) N - nucleus. (**b**, **c**) Corresponding confocal sections through the newly forming valve, showing (B) microtubules, and (**c**) both microtubules and silica (z stack, normal to pervalvar axis). Adapted from Tesson and Hildebrand (2010a). Reprinted with permission

of the areolae (Schmid 1980; Blank and Sullivan 1983; Cohn et al. 1989), and an abnormally curved shape of the frustule (Kharitonenko et al. 2015).

2.3.2 Actin Filaments

Fluorescence microscopy using suitably labeled probes (FITC-phallacidin, rhodamine-phalloidine) specific for actin filaments revealed a network surrounding the developing valve (Van de Meene and Pickett-Heaps 2004; Tesson and Hildebrand 2010a). In the centric diatoms *Cyclotella cryptica* and *C. granii*, an actin ring was observed right next to the propagating front of nascent biosilica (Fig. 9a–d) (Tesson and Hildebrand 2010a, b) (Fig. 9a). Superimposed fluorescent images of the developing valve and the actin filaments suggested that this actin ring defines the boundaries of the SDV (Fig. 9c, d), similar to observations in the pennate diatom *Surirella sp*. (Tesson and Hildebrand 2010a, b). The actin filaments associated with valve SDVs increased in size and density as valve morphogenesis progressed and displayed a meshwork at the proximal side of the valve SDV. In *T. pseudonana,* actin filaments were found to be located in close proximity to the developing girdle bands using ion-abrasion SEM imaging (Hildebrand et al. 2009). In *Entomoneis alata*, bundles of actin filaments were associated with one side of the girdle band SDV (Fig. 9e), and became completely rearranged after exocytosis (Fig. 9f) (Tesson and Hildebrand 2010a). Drugs that disrupt actin filaments affect morphogenesis of particular sub-structures of the frustule. In the centric *Rhizosolenia setigera*, cytochalasin D interfered with the development of labiate processes (Van de Meene and Pickett-Heaps 2004); in the pennate *Hantzschia amphioxys*, the same drug caused lateral displacement of the raphe canal from its submarginal position to the center of the valve (Cohn et al. 1989).

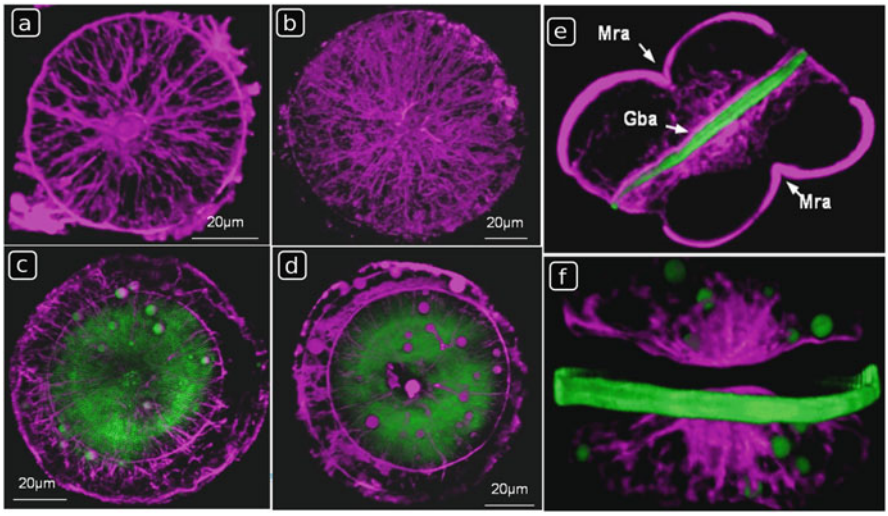

Fig. 9 Actin (purple) and silica (green) localization during valve and girdle band formation. Fluorescence microscopy was performed in (**a**–**d**) *C. granii* and (**e**, **f**) *Entomoneis alata*. (**a**) Actin network at an early stage of valve development. The actin ring is located at the front edge of the valve SDV and has not yet reached the cell periphery. (**b**) Actin network associated with the valve SDV at a late stage of development. (**c**, **d**) Overlay of actin and silica in the area of the valve SDV at an early developmental stage. Actin filaments (**e**) during girdle band formation, and (**f**) after exocytosis of the girdle band (girdle band view with the green labeled girdle band) SDV. Mra = mother cell raphe actin, Gba = girdle band actin. From Tesson and Hildebrand (2010a). Reprinted with permission

2.3.3 Putative Mechanisms for Cytoskeletal Control of Silica Morphogenesis

Although the results summarized above clearly demonstrate a role of the cytoskeleton in silica morphogenesis, the mechanisms by which this occurs remain unclear. The following scenarios seem feasible:

1. Positioning of the SDVs and controlling their expansion. To accomplish this, the cytoskeletal elements must establish physical contact with the SDV membrane through proteins that have specific affinity for both cytoskeletal elements and the cytoplasmic surface of the SDV membrane. Such proteins have not yet been discovered. Polymerizing actin filaments are known to impose mechanical tension in cells, which can trigger morphogenetic responses (Heisenberg and Bellaïche 2013), and microtubules and actin filaments are known to affect the shape of the membrane-based organelles in other systems (McMahon and Gallop 2005).
2. The cytoskeletal elements may interact with transmembrane proteins, which are located in the silicalemma and endowed with domains that promote silica formation in the SDV lumen. The patterns of microtubules and/or actin filaments at the

SDV surface would influence the positions of the silica-nucleating transmembrane proteins thereby guiding the formation of the silica patterns inside the SDV (Robinson and Sullivan 1987). Although occasionally the cytoskeleton patterns at the valve SDVs coincide with structural features of the patterns in mature silica (Tesson and Hildebrand 2010a, b), there is no clear evidence yet for the congruence of the patterns of cytoskeleton elements with nascent silica patterns during SDV biogenesis.

3. Actin filaments and microtubules may serve as tracks for motor protein-dependent transport of vesicles that deliver material for SDV expansion and function. The precise directions from which this material is delivered may be an important determinant of the morphogenesis mechanism.

Besides cytoskeleton elements intracellular organelles such as mitochondria, endoplasmic reticulum, and "spacer vesicles" have been implicated in valve morphogenesis in *Coscinodiscus wailesii*, *Achnantes longipes*, and *Pinnularia maior* (Schmid 1994). In TEM analysis of chemically fixed and embedded cells intracellular organelles appeared to act as "molding" matrices that shape the SDV and consequently affect the morphology of the silica being deposited inside the SDV. In this scenario differently sized vesicles and mitochondria associated with the SDV at different stages of valve morphogenesis might be templating the size and distribution of the pore patterns. An alternative model for pore morphogenesis in *Coscinosiscus* species assumes that dense hexagonal packings of long-chain polyamine containing droplets in the SDV lumen are responsible for both forming and molding the precipitating silica (Sumper 2002). Long-chain polyamines are ubiquitous in diatom silica (Kröger and Poulsen 2008; see also Chap. "Biomolecules Involved in Frustule Biogenesis and Function") and are known to generate appropriately sized droplets under physiologically relevant conditions *in vitro* (Bernecker et al. 2010).

3 Silica Morphogenesis

A prerequisite for developing a fundamental understanding of the mechanisms that drive silica morphogenesis in diatoms is detailed knowledge about intermediate stages of this process. For this purpose, cell cycle synchronization has often been used to strongly enrich the population with cells that are in the process of SDV development (Chiappino and Volcani 1977). In the past, two approaches have been principally applied to image developing silica: (1) Chemical fixation of the cells followed by resin embedding, ultrathin sectioning, and imaging by TEM (for review see Pickett-Heaps et al. 1990); in one case, sectioning and imaging was performed by ion abrasion and imaging by SEM (Hildebrand et al. 2009). (2) Isolation of the silica by treatment of the cells with mineral acids or detergents at elevated temperatures, and imaging of the silica structures with TEM, SEM, or atomic force microscopy (for review see Pickett-Heaps et al. 1990). The first method has the advantage that SDVs are imaged within their intact cellular context. However,

imaging the entire volume of a developing silica structure requires tedious serial sectioning and has only been reported once (Chiappino and Volcani 1977). With the second method, the entire volume of the developing silica structure can easily be imaged. However, the silica has been removed from the cellular context and subjected to harsh chemical treatment, which may have destroyed delicate, lightly silicified structures. Recently, a new method for imaging the structures of developing valves has been developed (Heintze et al. 2020). The method utilizes fluorescent labeling of valves in synchronized cells *in vivo* by briefly adding the acidotropic, fluorescent dye PDMPO to the cell culture, before any valve SDVs have been exocytosed. PDMPO accumulates in the SDV lumen, and becomes permanently entrapped within the nascent biosilica, but it does not stain mature biosilica on the cell surface (Shimizu et al. 2001). The labeled cells are gently lysed, the lysate spread on a TEM grid, the positions of valve SDVs quickly identified by fluorescence microscopy, and PDMPO labeled objects imaged by TEM. Although this method disrupts the cellular context of the developing valve SDV, the silica structures are still coated by the silicalemma and not subjected to artifact-prone chemical treatments. Therefore, it is expected that delicate silica structures are preserved (Heintze et al. 2020).

Irrespective of the method used for preparing and imaging the developing silica, a consistent picture has emerged regarding the early stages of silica morphogenesis. In both centrics and pennates, valve morphogenesis starts from a single silica center termed the primary silicification site (PSS) (Schmid and Schulz 1979), yet in both groups the morphology of the PSS is different. In centrics, it is a central ring (the annulus) from which branched ribs emerge, whereas in pennates it is a band of silica (the sternum). The morphological differences between the initial silica structures of centric and pennate diatoms already reflects the difference in valve symmetry between the two subgroups. In the following, we present examples that illustrate representative morphogenesis pathways in selected centric and pennate diatom species.

3.1 Valve Morphogenesis in Centrics

Thalassiosira pseudonana (from Heintze et al. 2020). Mature valves of *T. pseudonana* (Fig. 10a) possess a network of ribs that radiate from a central ring-like structure, called the *annulus* (Latin for ring). The radiating ribs occasionally branch, resulting in an approximately constant lateral spacing. The space between the ribs becomes filled with silica that contains numerous ~20 nm-sized cribrum pores. Neighboring ribs are linked by transversal silica bridges, resulting in an interconnected meshwork of silica ridges on the valve surface. Two neighboring silica bridges together with the interjacent segments of two neighboring ribs define an areola, which has a distorted rectangular shape. Fultoportulae are positioned equidistantly close to the rim of the valve, and about half of the valves also contain a central fultoportula.

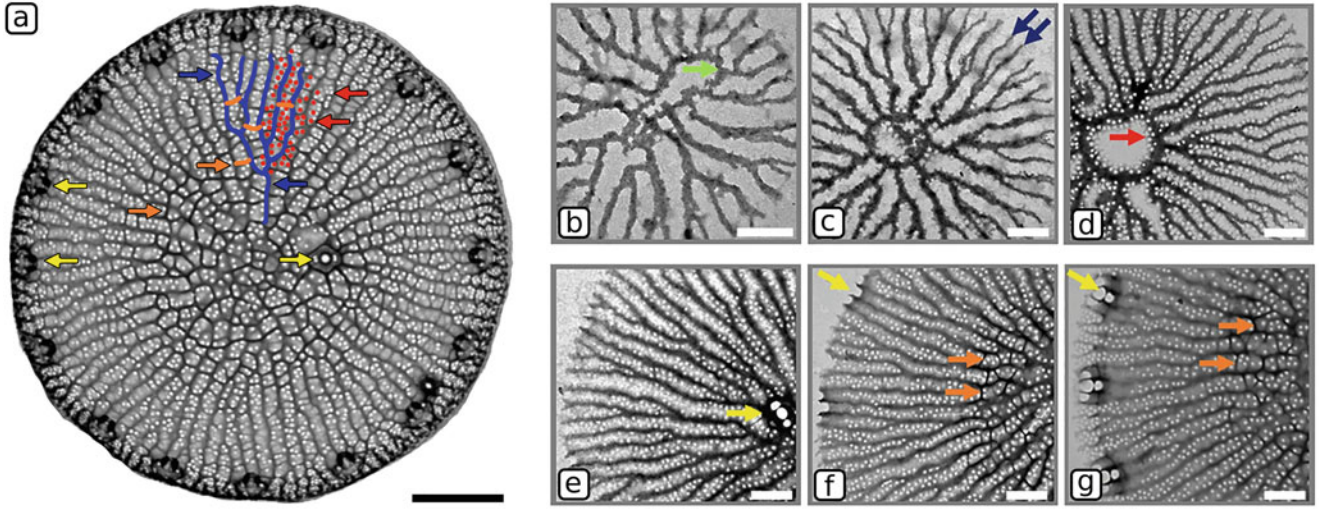

Fig. 10 Valve morphogenesis in *T. pseudonana*. (**a**) TEM image of a mature valve (courtesy of Stefan Görlich, TU Dresden). Arrows highlight characteristic biosilica features of the valve: green = annulus, blue = rib, red = cribrum pore, yellow = fultoportula, orange = areola pore. (**b–h**) For each developmental stage only part of the valve is shown. Scale bars: 1 µm (**a**), 400 nm (**b–g**). Adapted from Heintze et al. (2020)

At the earliest developmental stages found, the valves already consist of the annulus, from which regularly spaced short ribs extended radially outwards (Fig. 10b). The ribs continue growing radially and branch occasionally to fill the available space with approximately constant lateral spacing between neighboring ribs (Fig. 10c). Developing ribs possess rough edges and seem to be composed of an agglomeration of globular silica particles (Fig. 10c). Cribrum pores already form at the early stages of ribs outgrowth, initially close to the valve center (Fig. 10c, d). Subsequently, pore formation propagates radially outwards along the ribs. Concomitantly, a thin silica layer develops around the pores (Fig. 10e, f), which eventually fills the entire space between the ribs (Fig. 10g). When ribs have almost reached their full length, equidistantly spaced fultoportulae form synchronously near the rim of the developing valve. Fultoportula formation involves the ends of four (rarely three) ribs, which develop into one central tube with three satellite pores (Fig. 10g). The area immediately around the fultoportula is fully silicified and lacks cribrum pores. In the regions between the developing fultoportulae, ribs continue to extend, but stop shortly after fultoportulae formation is completed. Termination of lateral growth of the valve is marked by the ends of ribs merging into an unpatterned, nonporous ring of silica, which represents the margin of the mature valve (Fig. 10a).

The formation of branched ribs and the cribrum plate essentially represents two-dimensional growth within the valve plane. Growth in the perpendicular direction is referred to as *z*-expansion, and commences around the time when fultoportulae at the valve margin start to form. This phase involves completion of the fultoportulae, increase of rib height, and formation of silica bridges between neighboring ribs. Additionally, the ridges of ribs become endowed with linear arrays of globular silica nanoparticles (Hildebrand et al. 2006, 2018).

Coscinodiscus wailesii (from Schmid and Volcani 1983). The general arrangement of areola pores in the valve of *C. wailesii* is similar to *C. centralis* (see Fig. 4e). Specifically, the valve comprises two parallel silica layers, which are connected by areolar walls that are arranged in a honeycomb pattern. As a consequence, the valve has a chambered structure as in *C. centralis* (see Fig. 4d). The proximal silica layer contains the foramina and the distal layer the cribrum pores. Valve morphogenesis begins with formation of the foramen layer, presumably by the aggregation of spherical silica particles that connect into long strands extending from the valve center (Fig. 11a). As valve formation progresses, these strands engulf circular domains devoid of silica, which subsequently develop into areola pores (Fig. 11b, c). There is a gradient of valve maturation as a function of radial distance from the valve center, with the more mature structures being closer to the valve center. While the foramen layer is still expanding in the *xy*-plane, the areola walls grows in *z*-direction (Fig. 11d). After reaching their final height, the areola walls develop regularly spaced teeth-like extensions (Fig. 11e). The silica teeth then grow radially inward to the center of each areola pore (Fig. 11f), thus sub-dividing each areola pore into smaller cribrum pores (Fig. 11g). Concomitantly, the space between cribrum pores becomes filled with an additional silica layer with even smaller pores (cribrellum, not shown here).

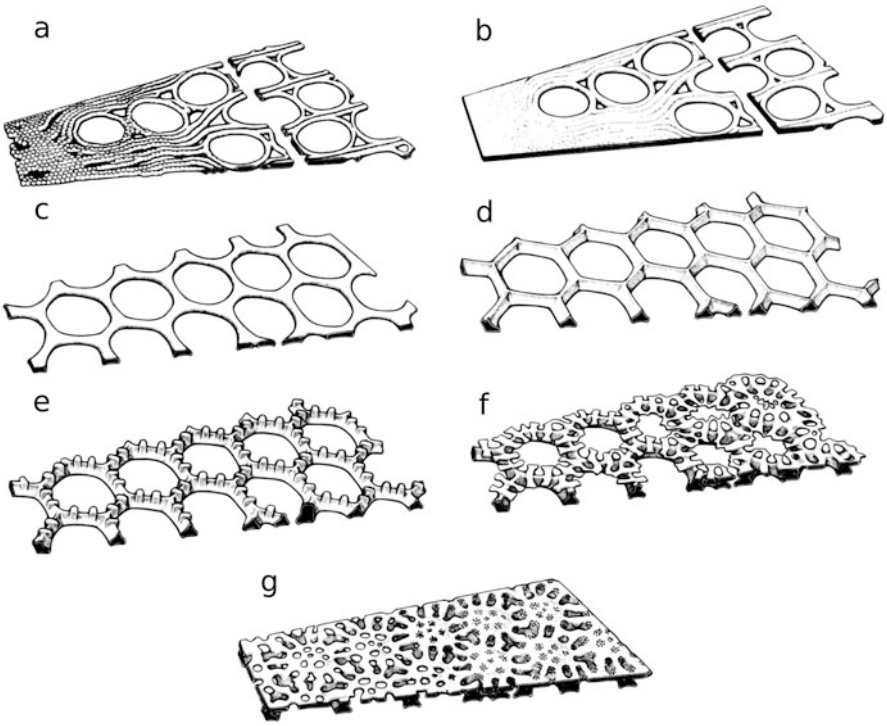

Fig. 11 Schematic of valve formation in *Coscinodiscus wailesii*. (**a**) Initial deposition of silicified strands and formation of the foramen layer. (**b**) Smoothing of deposited biosilica close to the valve center. (**c**) Foramen layer with foramen openings of the future areola pores. (**d**) Perpendicular growth of the areola walls. (**e**) Growth of regularly spaced silicified "teeth" on the areola walls. (**f**–**g**) Lateral expansion of aforementioned silica teeth, establishing the cribrum layer interspersed by cribrum pores. Adapted from Schmid and Volcani (1983). Reprinted with permission

Plagiogrammopsis vanheurckii (from Sato 2010). This species is a bipolar centric diatom with each of its valves comprising a single silica layer shaped like a lance head (Fig. 12a). The valves contain numerous areola pores, which are occluded by a cribrum layer. The earliest stage of valve development that could be imaged consisted of a thin silica layer comprising a ring-shaped pattern center (annulus) and radiating silica ribs (Fig. 12b). The ribs branch into dendritic trees, and at a certain distance from the annulus, fuse into a smooth silica surface interspersed by developing areola pores (Fig. 12b). The areolae form by the merging of two silica ribs that engulf a circular region (Fig. 12c) and subsequently merge to form a smooth pore boundary (Fig. 12d–f).

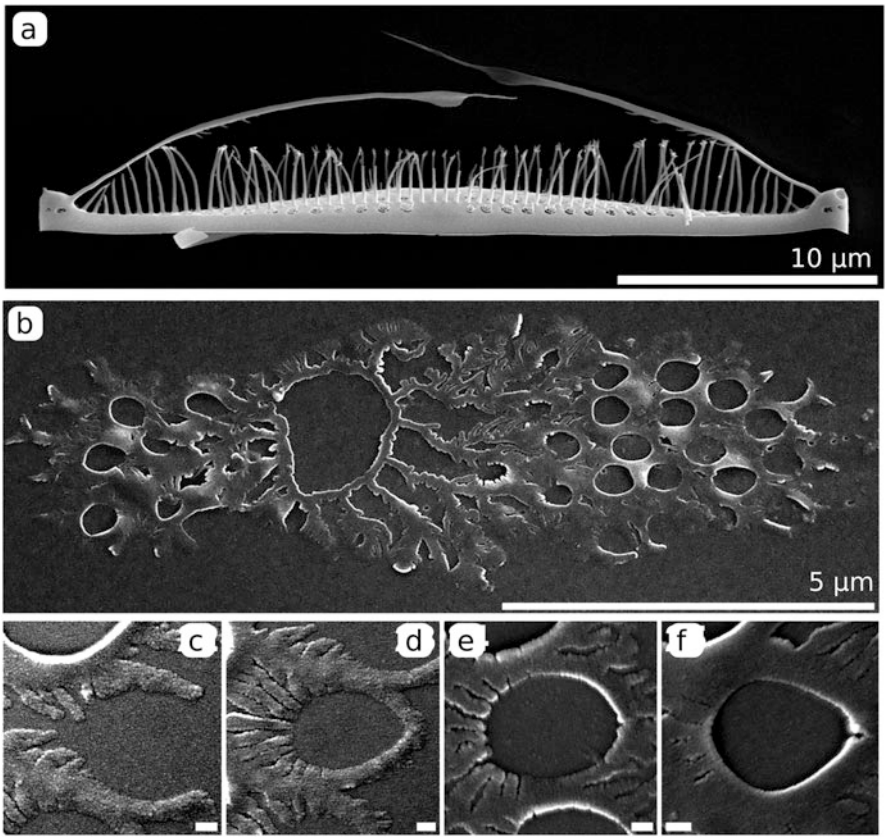

Fig. 12 SEM images of valve formation in *P. vanheurckii*. (**a**) Mature valve. (**b**) The earliest observed stages of valve morphogenesis. (**c**–**f**) Sequential stages of areola pore formation by merging silica ribs. Scale bars: 0.5 µm. Adapted from Sato (2010). Reprinted with permission

3.2 Valve Morphogenesis in Pennates

To date, valve morphogenesis in pennates has mostly been studied in raphid species and much less in araphids. Morphogenesis of raphid valves and araphid valves appears to be fundamentally identical. It starts with establishing the apical axis by forming the sternum (further developing into the raphe in raphids) followed by transapical valve development. Here, we describe morphogenesis of both a nonchambered valve and a chambered valve from two raphid pennates. Examples of araphid valve morphogenesis are provided elsewhere (Crawford and Schmid 1986; Tiffany 2002; Kaluzhnaya and Likhoshway 2007; Sato et al. 2011, and Kharitonenko et al. 2015).

"Navicula pelliculosa" (from Chiappino and Volcani 1977). This species was originally misidentified (Schoeman et al. 1976) and now is named *Adlafia minuscula*

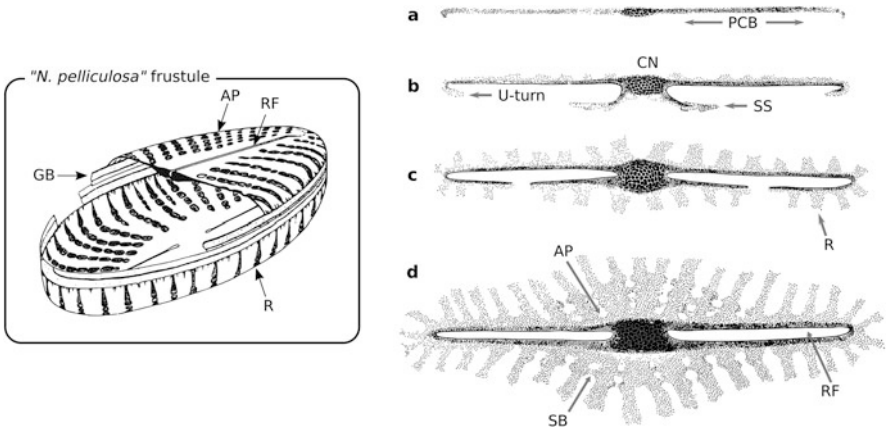

Fig. 13 Valve morphogenesis in "*N. pelliculosa*". (left) Schematic of the frustule. (**a**–**d**) Early stages of development. PCB = primary central band; CN = central nodule; SS = secondary strands; RF = future raphe; R = rib; AP = areola pore; SB = silica bridges. Adapted from Volcani (1981), Chiappino and Volcani (1977). Reprinted with permission

var. muralis (Lange-Bertalot 1999). However, as this species is still widely referred to under its original name, we will use it here in quotes. "*N. pelliculosa*" valves have an elliptical shape with a raphe system running along the apical axis. Near the tips of each valve, the ends of the raphe slits bend towards the girdle band region. The valve has a characteristic array of pores that are organized in parallel rows (striae) that extend from both sides of the raphe (Fig. 13, left). The earliest developmental stage observed is a continuous band of biosilica termed primary central band (PCB) consisting of a heavily silicified central structure (central nodule, CN) and extending primary strands. After the PCB has reached its full length, its two tips start to curve back towards the CN position on both sides, forming U-turns (Fig. 13b). Simultaneously, an additional pair of strands (secondary strands) outgrow from the CN, extending towards the U-turns (Fig. 13b, c). The primary and secondary strands elongate, and eventually merge, thus enclosing the future raphe slits (Fig. 13c, d). In some raphid pennates, the point of strand merger can be still seen in mature valves as a small interruption in the stria pattern, which is termed the Voigt discontinuity (Mann 1981). Already before primary and secondary strands merge, transapically oriented ribs emerge with equidistant spacing along the entire length of both strands. At first, these ribs grow in length but not in width, but then regularly spaced silica bridges form between neighboring ribs, thereby establishing a regular pattern of future areola pores. Finally, these areolae become occluded by a thin silica layer perforated by regularly arranged cribrum pores. The formation of cribrum pores is described in more detail below for *Diploneis smithii*. The ribs in pennate valves can be considered analogous to radiating ribs in centrics. However, during development of centric valves all ribs grow from the pattern center simultaneously with the same speed, whereas in pennates ribs closer to the apical ends grow slower than those near the central nodule. How this gradient of rib growth rates is established is unknown.

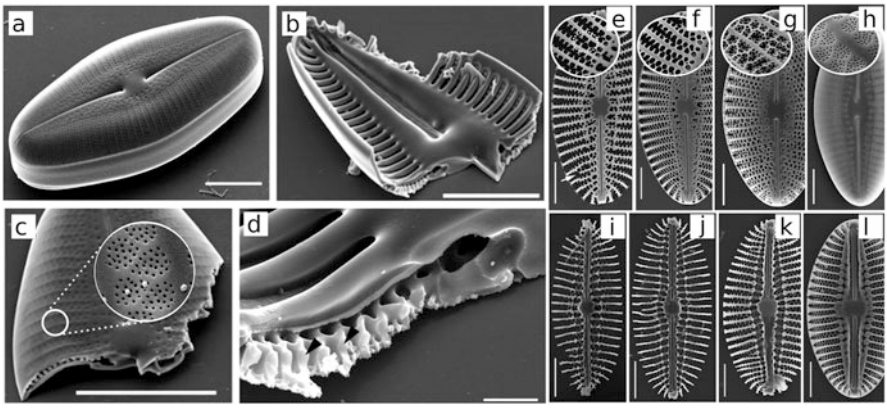

Fig. 14 SEM images of the *Diploneis smithii* frustule in (**a**–**d**) the mature stage and (**e**–**l**) during development. (**a**) Oblique view of the entire frustule. (**b**) Proximal surface of theca fragment, showing the raphe and heavily silicified transapical ribs. (**c**) Distal surface. Inset: cribrum pore pattern. (**d**) At the fracture edge, the chambered architecture of the two-layered valve is visible, with the walls of the areola pores serving as struts that connect the proximal and distal layers of the valve. (**e**–**h**) Distal view. Outgrowth of spines perpendicular to the ribs that branch and merge, thus establishing a pattern of areolae pores. (**i**–**l**) Proximal view. The raphe sternum and the bases of ribs thicken bordering the central raphe canal and the alveoli, respectively. Scale bars: 10 μm (**a**–**c**), 1 μm (**d**), 5 μm (**e**–**l**). Adapted from Idei et al. (2018). Reprinted with permission

Diploneis smithii (form Idei et al. 2018). Species of the genus *Diploneis* possess one of the most intricate valve structures among all pennates. The oval valves have a two-layered, chambered architecture with distinct morphology of distal and proximal layers (Fig. 14a–c).

The distal surface of the valve possesses regularly spaced groups of areolae that are occluded with a cribrum layer containing ~20 pores (Fig. 14c). The proximal side has a central canal with the raphe at its center and a series of regularly spaced transapical canals separated by heavily silicified ribs (Fig. 14d). The early stages of valve development in *D. smithii* are identical to those in *N. pelliculosa* with one exception: silica bridges between neighboring ribs are branched rather than straight lines (Fig. 14e, f). The branched silica bridges delineate areola pores, inside which patterns of cribrum pores form. This is achieved by the inward growth and subsequent fusion of thin spine-like structures protruding from the areola walls (Fig. 14g, h). While the ribs grow outwards (in the *xy*-plane), the base layer of the valve expands proximally in *z*-direction, which leads to a thickening of the raphe sternum and the bases of the ribs. As a result, a heavily silicified central raphe canal is produced as well as elongated holes, termed *alveoli* (from Latin trough), which are positioned on the proximal side of the valve underneath the areolae (Fig. 14i–l).

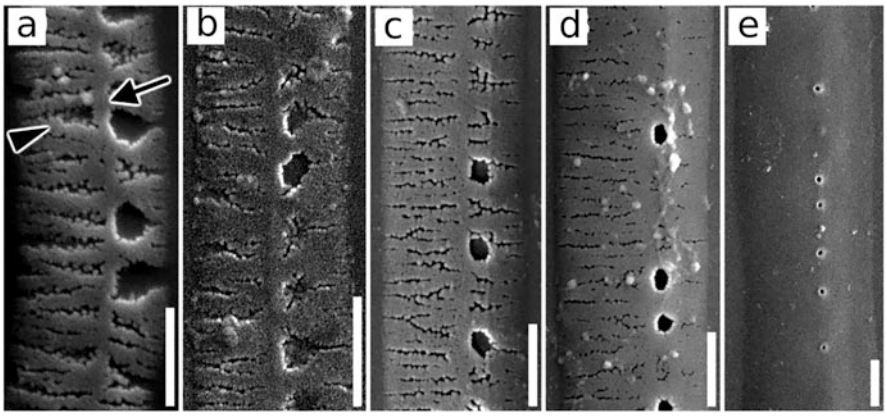

Fig. 15 SEM images of girdle band morphogenesis in *P. vanheurckii*. Images are ordered to indicate the gradual progression from the earliest observable stage (**a**) through intermediate stages (**b-d**) to a mature structure (**e**). Early stages of girdle band formation comprised a longitudinal rib (arrow) and lateral branches (arrowhead). Scale bar: 1.5 μm. From Sato (2010). Reprinted with permission

3.3 Girdle Band Morphogenesis

To date, studies on girdle band morphogenesis are rare, because intermediate developmental stages are more difficult to identify than for the much more massive structures of the valves. Two recent studies investigated girdle band morphogenesis in the bipolar centrics *Isthmia nervosa* (Tiffany 2005) and *Plagiogrammopsis vanheurckii* (Sato 2010). The earliest observable stages of girdle band morphogenesis in *P. vanheurckii* exhibited a central longitudinal rib with lateral branches perpendicular to the rib (Fig. 15a). Each branch appears to be assembled from globular silica nanoparticles with diameters of about 20 nm. The branches increase in thickness (Fig. 15b, c) until the gaps between neighboring branches are filled with silica, except for a few domains that are destined to become areola pores in the mature girdle band (Fig. 15d, e).

It was pointed out (Sato 2010) that girdle band morphogenesis in bipolar centrics resembles morphogenesis to the primary rib system in araphid pennates (Tiffany 2002; Kaluzhnaya and Likhoshway 2007), which suggests that similar mechanisms might apply.

4 Conclusion

Despite an apparent multitude of frustule morphogenesis pathways, there seem to be at least two fundamental principles that apply to most (if not all) diatom subgroups:

1. Valve and girdle band morphogenesis are spatially (distinct SDVs) and temporally (cell division vs. interphase) separated events;
2. Silica morphogenesis originates from a single nucleation center inside the SDV rather than multiple nucleation sites. This principle applies even to the most complex valve architectures.

The second principle sets the initial condition of morphogenesis, which constrains possible theoretical models. Previous theoretical work considered diffusion-limited aggregation models (Parkinson et al. 1999), phase separation models (Lenoci and Camp 2008), or stochastic aggregation models with lateral feedback to account for pore occlusions (Willis et al. 2013). These theoretical models partially reproduce key features of mature valve patterns of certain model diatoms, yet do not reproduce the time-course of morphogenesis, such as regular radial rib patterns during valve formation, which occurs in a vast number of diatom species. Several models sought to explain the role of silica-associated biomacromolecules in silica morphogenesis including silaffins and long-chain polyamine-based in terms of a phase separation processes (Sumper 2002; Vrieling et al. 2002). On a smaller scale, theoretical models addressed the formation of areola patterns while assuming a given pre-pattern of ribs (Lenoci and Camp 2008). Recently, separate patterning mechanisms for different structural features were combined into a single, more holistic model (Bobeth et al. 2020). Despite these advances, we are only beginning to understand the dynamics of silica morphogenesis and the underlying physical mechanisms, let alone the genetic mechanisms that control the diversity of observed patterns.

Acknowledgements We would like to thank David Mann (Royal Botanic Garden Edinburgh, UK) and Shinya Sato (Fukui Prefectural University, Japan) for critically reading the manuscript. We are indebted to the Deutsche Forschungsgemeinschaft (DFG) for financial support through grants KR1853/6-2 and KR1853/8-2 (to NK) in the framework of Research Unit 2038 (NANOMEE), and through a "Physics of Life" Starting Grant under Germany's Excellence Strategy – EXC-2068 – 390729961– Cluster of Excellence Physics of Life of TU Dresden (to NK and BMF). BMF acknowledges support by the DFG through a Heisenberg grant (FR3429/4-1).

References

Bedoshvili Y, Gneusheva K, Popova M, Morozov A, Likhoshway Y (2018) Anomalies in the valve morphogenesis of the centric diatom alga *Aulacoseira islandica* caused by microtubule inhibitors. Biol Open 7:bio035519

Bernecker A, Wieneke R, Riedel R, Seibt M, Geyer A, Steinem C (2010) Tailored synthetic polyamines for controlled biomimetic silica formation. J Am Chem Soc 132:1023–1031

Bishop I, Spaulding S (2014) Diatoms of North America. The source for diatom identification and ecology. https://diatoms.org/

Blank GS, Sullivan CW (1983) Diatom mineralization of silicic acid. VII. Influence of microtubule drugs on symmetry and pattern formation in valves of *Navicula saprophila* during morphogenesis. J Phycol 19:294–301

Bobeth M, Dianat A, Gutierrez R, Werner D, Yang H, Eckert H, Cuniberti G (2020) Continuum modelling of structure formation of biosilica patterns in diatoms. BMC Mater 2:1–11

Bradbury J (2004) Nature's nanotechnologists: unveiling the secrets of diatoms. PLoS Biol 2(10): e306
Chiappino ML, Volcani BE (1977) Studies on the biochemistry and fine structure of silicia shell formation in diatoms VII. Sequential cell wall development in the pennate *Navicula pelliculosa*. Protoplasma 93:205–221
Cohn SA, Nash J, Pickett-Heaps JD (1989) The effect of drugs on diatom valve morphogenesis. Protoplasma 149:130–143
Crawford RM, Schmid AM (1986) Ultrastructure of silica deposition in diatoms. In: Leadbeater BS, C., Riding R. (eds) Biomineralization in lower plants and animals. Clarendon Press, Oxford, pp 291–314
Dawson PA (1973) Observations on the structure of some forms of *Gomphonema parvulum*. Kütz. III. Frustule formation. J Phycol 9:165–175
Drum RW, Pankratz HS (1964) Post mitotic fine structure of Gomphonema parvulum. J Ultrastruct Res 10:217–223
Durkin CA, Mock T, Armbrust EV (2009) Chitin in diatoms and its association with the cell wall. Euk Cell 8:1038–1050
Eppley RW, Holmes RW, Strickland JD (1967) Sinking rates of marine phytoplankton measured with a fluorometer. J Exp Mar Biol Ecol 1:191–208
Geitler L (1932) Der Formwechsel der pennaten Diatomeen. Archiv fur Protistenkunde 78:1–226
Girard V, Saint Martin S, Saint Martin JP, Schmidt AR, Struwe S, Perrichot V, Breton G, Néraudeau D (2009) Exceptional preservation of marine diatoms in upper Albian amber. Geology 37(1):83–86
Gladenkov AY (2012) Middle Eocene diatoms from the marine Paleogene stratigraphic key section of Northeast Kamchatka. Austrian J Earth Sci 105:1
Heintze C, Formanek P, Pohl D, Hauptstein J, Rellinghaus B, Kröger N (2020) An intimate view into the silica deposition vesicles of diatoms. BMC Mater. 2:1–15
Heisenberg CP, Bellaïche Y (2013) Forces in tissue morphogenesis and patterning. Cell 153:948–962
Herth W, Schnepf E (1982) Chitin-fibril formation in algae. In: Cellulose and other natural polymer systems. Springer, Boston, MA, pp 185–206
Hildebrand M, York E, Kelz JI, Davis AK, Frigeri LG, Allison DP, Doktycz MJ (2006) Nanoscale control of silica morphology and three-dimensional structure during diatom cell wall formation. J Mater Res 21:2689–2698
Hildebrand M, Frigeri LG, Davis AK (2007) Synchronized growth of *Thalassiosira pseudonana* (bacillariophyceae) provides novel insights into cell wall synthesis processes in relation to the cell cycle. J Phycol 43:730–740
Hildebrand M, Kim S, Shi D, Scott K, Subramaniam S (2009) 3D imaging of diatoms with ion-abrasion scanning electron microscopy. J Struct Biol 166:316–328
Hildebrand M, Lerch SJ, Shrestha RP (2018) Understanding diatom cell wall silicification—moving forward. Front Mar Sci 5:125
Hoops HJ, Floyd GL (1979) Ultrastructure of the centric diatom, *Cyclotella meneghiniana*: vegetative cell and auxospore development. Phycologia 18(4):424–435
Idei M, Sato S, Tamotsu N, Mann DG (2018) Valve morphogenesis in *Diploneis smithii* (Bacillariophyta). J Phycol 54:171–186
Kaluzhnaya OV, Likhoshway YV (2007) Valve morphogenesis in an araphid diatom *Synedra acus subsp. radians*. Diatom Res 22:81–87
Kharitonenko KV, Bedoshvili YD, Likhoshway YV (2015) Changes in the micro-and nanostructure of siliceous valves in the diatom *Synedra acus* under the effect of colchicine treatment at different stages of the cell cycle. J Struct Biol 190:73–80
Kotzsch A, Gröger P, Pawolski D, Bomans PH, Sommerdijk NA, Schlierf M, Kröger N (2017) Silicanin-1 is a conserved diatom membrane protein involved in silica biomineralization. BMC Biol 15:1–16

Kröger N, Poulsen N (2008) Diatoms - from cell wall biogenesis to nanotechnology. Annu Rev Genet 42:83–107
Lange-Bertalot H (1999) Diatoms from Siberia I. Islands in the Arcic Ocean (Yugorsky Shar Strait). Iconographia Diatomologica 6:273
LeDuff P, Rorrer GL (2019) Formation of extracellular β-chitin nanofibers during batch cultivation of marine diatom *Cyclotella sp*. at silicon limitation. J Appl Phycol 31:3479–3490
Lenoci L, Camp PJ (2008) Diatom structures templated by phase-separated fluids. Langmuir 24: 217–223
Mann DG (1981) A note on valve formation and homology in the diatom genus *Cymbella*. Ann Bot 47:267–269
McMahon HT, Gallop JL (2005) Membrane curvature and mechanisms of dynamic cell membrane remodelling. Nature 438:590–596
Medlin LK, Crawford RM, Andersen RA (1986) Histochemical and ultrastructural evidence for the function of the labiate process in the movement of centric diatoms. Br Phycol J 21:297–301
Moore ER, Bullington BS, Weisberg AJ, Jiang Y, Chang J, Halsey KH (2017) Morphological and transcriptomic evidence for ammonium induction of sexual reproduction in *Thalassiosira pseudonana* and other centric diatoms. PLoS One 12:e0181098
Nagai S, Hori Y, Manabe T, Imai I (1995) Restoration of cell size by vegetative cell enlargement in *Coscinodiscus wailesii* (Bacillariophyceae). Phycologia 34:533–535
Parkinson J, Brechet Y, Gordon R (1999) Centric diatom morphogenesis: a model based on a DLA algorithm investigating the potential role of microtubules. Biochem Biophys Acta 1452:89–102
Pickett-Heaps JD, Tippit DH, Andreozzi JA (1979) Cell division in the pennate diatom Pinnularia. IV. Valve morphogenesis. Biol Cell 35:295
Pickett-Heaps JD, Schmid AMM, Edgar LA (1990) The cell biology of diatom valve formation. In: Round FE, Chapman DJ (eds) Progress in psychological research. Biopress, Bristol, pp 1–168
Robinson DH, Sullivan CW (1987) How do diatoms make silicon biominerals? Trends Biochem Sci 12:151–154
Romann J, Valmalette JC, Chauton MS, Tranell G, Einarsrud MA, Vadstein O (2015) Wavelength and orientation dependent capture of light by diatom frustule nanostructures. Sci Rep 5:1–6
Round FE, Crawford RM, Mann DG (1990) Diatoms: biology and morphology of the genera. Cambridge University Press, Cambridge
Sar EA, Sunesen I, Jahn R (2010) *Coscinodiscus perforatus* revisited and compared with *Coscinodiscus radiatus* (Bacillariophyceae). Phycologia 49:514–524
Sato S (2010) Valve and girdle band morphogenesis in a bipolar centric diatom *Plagiogrammopsis vanheurckii* (Cymatosiraceae, Bacillariophyta). Eur J Phycol 45:167–176
Sato S, Medlin LK (2006) Motility of non-raphid diatoms. Diatom Res 21:473–477
Sato S, Mann DG, Nagumo T, Tanaka J, Tadano T, Medlin LK (2008) Auxospore fine structure and variation in modes of cell size changes in *Grammatophora marina* (Bacillariophyta). Phycologia 47:12–27
Sato S, Watanabe T, Nagumo T, Tanaka J (2011) Valve morphogenesis in an araphid diatom *Rhaphoneis amphiceros* (Rhaphoneidaceae, Bacillariophyta). Phycol Res 59:236–243
Schmid AMM (1980) Valve morphogenesis in diatoms: a pattern-related filamentous system in pennates and the effect of APM, colchicine and osmotic pressure. Nova Hedw 33:811–847
Schmid AMM (1994) Aspects of morphogenesis and function of diatom cell walls with implications for taxonomy. In: The protistan cell surface. Springer, Vienna, pp 43–60
Schmid AMM, Schulz D (1979) Wall morphogenesis in diatoms: deposition of silica by cytoplasmic vesicles. Protoplasma 100:267–288
Schmid AMM, Volcani BE (1983) Wall morphogenesis in *Coscinodiscus wailesii* Gran and Angst. I. Valve morphology and development of its architecture. J Phycol 19:387–402
Schmid AMM, Borowitzka MA, Volcani BE (1981) Morphogenesis and biochemistry of diatom cell walls. In: Cytomorphogenesis in plants. Springer, Vienna, pp 63–97
Schoeman FR, Archibald REM, Barlow DJ (1976) Structural observations and notes on the freshwater diatom *Navicula pelliculosa* (Brébisson ex Kützing) Hilse. Br Phycol J 11:251–263

Schulz D, Drebes G, Lehmann H, Jank-Ladwig R (1984) Ultrastructure of Anaulus creticus Drebes & Schulz with special reference to its reduced ocelli. Eur J Cell Biol 33:43–51
Shimizu K, Del Amo Y, Brzezinski MA, Stucky GD, Morse DE (2001) A novel fluorescent silica tracer for biological silicification studies. Chem Biol 8:1051–1060
Simpson TL, Volcani BE (eds) (2012) Silicon and siliceous structures in biological systems. Springer, New York
Sims PA, Mann DG, Medlin LK (2006) Evolution of the diatoms: insights from fossil, biological and molecular data. Phycologia 45:361–402
Spaulding S, Potapova M (2020). Diatoms of North America. The source for diatom identification and ecology. https://diatoms.org/
Sumper M (2002) A phase separation model for the nanopatterning of diatom biosilica. Science 295:2430–2433
Tesson B, Hildebrand M (2010a) Extensive and intimate association of the cytoskeleton with forming silica in diatoms: control over patterning on the meso-and micro-scale. PLoS One 5: e14300
Tesson B, Hildebrand M (2010b) Dynamics of silica cell wall morphogenesis in the diatom *Cyclotella cryptica*: substructure formation and the role of microfilaments. J Struct Biol 169: 62–74
Tesson B, Lerch SJ, Hildebrand M (2017) Characterization of a new protein family associated with the silica deposition vesicle membrane enables genetic manipulation of diatom silica. Sci Rep 7: 1–13
Tiffany MA (2002) Valve morphogenesis in the marine araphid diatom *Gephyria media* (Bacillariophyceae). Diatom Res 17:391–400
Tiffany MA (2005) Diatom auxospore scales and early stages in diatom frustule morphogenesis: their potential for use in nanotechnology. J Nanosci Nanotechnol 5:131–139
Van De Meene AM, Pickett-Heaps JD (2002) Valve morphogenesis in the centric diatom *Proboscia alata* Sundstrom. J Phycol 38:351–363
Van de Meene AM, Pickett-Heaps JD (2004) Valve morphogenesis in the centric diatom *Rhizosolenia setigera* (Bacillariophyceae, Centrales) and its taxonomic implications. Eur J Phycol 39:93–104
Volcani BE (1981) Cell wall formation in diatoms: morphogenesis and biochemistry. In: Silicon and siliceous structures in biological systems. Springer, New York, pp 157–200
Vrieling EG, Gieskes WWC, Beelen TP (1999) Silicon deposition in diatoms: control by the pH inside the silicon deposition vesicle. J Phycol 35:548–559
Vrieling EG, Beelen TP, van Santen RA, Gieskes WW (2002) Mesophases of (bio) polymer–silica particles inspire a model for silica biomineralization in diatoms. Angew Chem Int Ed 41:1543–1546
Walsby AE, Xypolyta A (1977) The form resistance of chitan fibres attached to the cells of Thalassiosira fluviatilis Hustedt. Br Phycol J 12:215–223
Wetzel CE, Ector L (2014) Taxonomy, distribution and autecology of *Planothidium bagualensis sp. nov.*(Bacillariophyta) a common monoraphid species from southern Brazilian rivers. Phytotaxa 156:201–210
Willis L, Cox EJ, Duke T (2013) A simple probabilistic model of submicroscopic diatom morphogenesis. J R Soc Interf 10:20130067
Yee DP, Hildebrand M, Tresguerres M (2020) Dynamic subcellular translocation of V-type H^+-ATPase is essential for biomineralization of the diatom silica cell wall. New Phytol 225:2411–2422
Zurzolo C, Bowler C (2001) Exploring bioinorganic pattern formation in diatoms. A story of polarized trafficking. Plant Physiol 127:1339–1345